World Journal of Advanced Engineering Technology and Sciences
eISSN: 2582-8266
Cross Ref DOI: 10.30574/wjaets
Journal homepage: https://wjaets.com/

(REVIEW ARTICLE)

Check for updates

Precision of the transfer function estimation of analog-to-digital converters in the presence of additive noise

Francisco André Corrêa Alegria *

Instituto de Telecomunicações and Instituto Superior Técnico, University of Lisbon, Portugal.

World Journal of Advanced Engineering Technology and Sciences, 2023, 10(01), 136–146

Publication history: Received on 15 August 2023; revised on 02 October 2023; accepted on 05 October 2023

Article DOI: https://doi.org/10.30574/wjaets.2023.10.1.0266

Abstract

Analog-to-digital converters are essential components in modern systems which gather data from the real world to be used, after signal processing, in many ubiquitous applications. This work addresses the effect of the presence of additive noise in the test setup when characterizing these electronic devices using the Histogram Test method. The precision with which the converter transfer function is estimated is directly related to the amount of noise present, the number of data samples acquired and the sinusoidal stimulus signal amplitude. Here an analytical expression that quantifies this precision as a function of the test parameters is given to be used by the engineer when designing the test.

Keywords: Histogram test method; Analog-to-digital conversion; Noise; Precision

1. Introduction

In the information age that we live in, the paramount commodity is data. In all kinds of devices, we find around us, from cars and mobile phones to houses, offices and factories, the gathering, storing, and processing of a myriad of signals is a happening without us being aware. For all those systems, which tend to be highly complex, to operate as expected without user intervention, they need to be very well designed. The signal measurements that underlie all this are nowadays carried out by a canonical system made up of sensors that "measure" everything in our environment, analog-to-digital converters (ADCs) that transform the signals created into digital words which can then be easily transmitted and stored without practically any loss of information and through unimaginable distances.

Those ADCs [1]-[2] are part of what we call an acquisition system with a certain signal conditioning circuitry, voltage range, sampling frequency and number of bits [3]-[4]. Naturally the behavior of those systems, in particular the accuracy of signal representation, is closely related to how they are implemented. Being electronic circuits, they are subject to all kinds of non-ideal phenomena like lack of linearity, spurious interference, additive noise, phase noise in sampling frequency oscillator, jitter in the sampling instants, etc. The engineer way to deal with all these phenomena is, for one, to use the Fourier theory and decompose the signals involved into a sum of sinewaves. The behavior of the system under those sinewaves can then be studied more easily and the effect of those non-ideal phenomena accounted for like the creation of spurious frequency components due to the nonlinear behavior of the acquisition system [5], uncertainty on the estimation of sinusoidal parameters due to the presence of additive noise [6]-[7], jitter in the sampling instant [8]-[9] or frequency error on the signals [10]-[11]. Note that the use of sinusoidal signals is generalized in engineering going well beyond acquisition system characterization. They are used, for example, in geophysical exploration [12], liquid fluid velocity measurement [13]-[15], sonar [16] and distance measurement [17], just to name a few.

This work addresses one of those problems, namely the non-linearity of the ADC behavior which can be corrected if properly characterized. The most common method to do so is the Histogram Test Method, also known as the Code

* Corresponding author: Francisco André Corrêa Alegria

Density Method [18]-[22], in particular for the determination of the transition voltages [23]-[24]. This method consists in applying a sinusoidal stimulus signal to the ADC and acquiring a very large number of samples. If the ADC had an ideal behavior, the number of samples with each of the possible ADC output codes would be exactly the one predicted theoretically, for that shape of stimulus. Any deviation in the number of counts of the histogram or, more commonly, the cumulative histogram, allows for an easy estimation of the actual value of the transition voltages. Those values are naturally only an estimative and are affected by the random effects present like noise and jitter. The transition voltage estimators will thus have a certain variance and bias that one wants to be as small as possible, hence the use of a large number of samples. The use of stimulus signals with different temporal evolutions like triangular ones [25] of even noise [26]-[28] has been proposed and studied in the past. It just leads to a different expected output code distribution.

2. Histogram Test Method

The transfer function of an ADC relates the input voltage with the digital output word. Different ADCs have different number of bits (n_b) and output word size. In the example shown in Figure 1 there are eight different possible output codes which are represented using three bits (numbered from 0 to $2^{n_b}-1$). We thus have the transfer function of a 3-bit ADC.

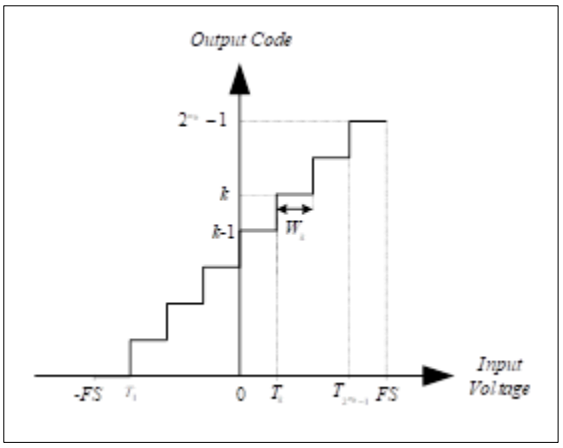

Figure 1 Transfer function of an ADC with n_b-bits. In this example n_b is 3

The value of the input voltage at which the output transitions from output code $k-1$ to output code k is called the transition voltage T_k. The difference between two consecutive transition voltages is the code bin width

$$W_k = T_{k+1} - T_k \, , k = 1 \ldots 2^{n_b} - 2 \ldots\ldots\ldots\ldots\ldots\ldots (1)$$

In the example given in Figure 1 we have a bipolar ADC, that is, one where the input voltage can be positive or negative. The limits of the input range, called "Full-scale" are $-FS$ and FS. There are other transfer function definitions where the transition voltages are not symmetric or even where they are all positive (unipolar ADC) [29]-[30].

To carry out the test a sinewave that covers the entire ADC range is applied (v_{in}). It has a properly chosen amplitude (A), offset (C), frequency (f) and initial phase (φ):

$$v_{in}(t) = C - A \cdot \cos(2\pi f \cdot t + \varphi). \ldots\ldots\ldots\ldots\ldots\ldots (2)$$

This signal is applied to the ADC and sampled at a constant rate, the sampling frequency f_s leading to a set of M sampling instants t_i at

$$t_i = \frac{i}{f_s} \, , i = 0, 1, \ldots, M-1. \ldots\ldots\ldots\ldots\ldots\ldots (3)$$

The samples are acquired, and a histogram of the 2^{n_b} possible output codes is computed like the one illustrated in Figure 2. The vertical bar height, h_k, corresponds to the number of samples that have a specific code k

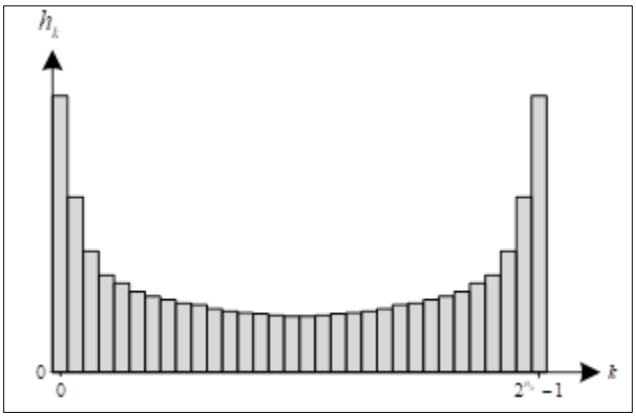

Figure 2 Example of an output sample histogram. In this example there are 16 bins corresponding to a 4-bit ADC

The lower and higher output codes happen more often because the sinusoidal signal voltage does not change linearly with time. It is more often "encountered" at the maximum or minimum. This example is for an 4-bit ADC which has 16 different possible output codes.

From this histogram the cumulative histogram, c_k, is computed by counting the number of samples that have an output code k or lower. The example shown in Figure 3, corresponds to the same case as in Figure 2. We see that the value of the last bin of the cumulative histogram always has a value equal to the number of samples acquired, M.

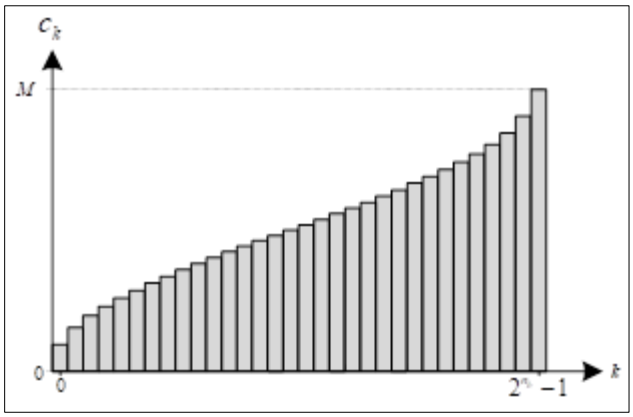

Figure 3 Example of an output sample cumulative histogram. In this example there are 16 bins corresponding to a 4-bit ADC

If the ADC behaves ideally, the number of codes in each bin k will have a known value. If the ADC does not have an ideal transfer function, the number of output codes in each bin will vary. If there is noise in the input voltage, on the sampling clock signal or on the ADC itself, the number of codes in each bin will be random.

The estimated transition voltages are given by

$$\hat{T}_k = C - A \cdot \cos\left(\frac{c_{k-1}}{M}\right), k = 1, 2, \dots, 2^{n_b} - 1. \quad \text{.....(4)}$$

Note the "hat" symbol over the transition voltage variable indicating that it is an estimated value. Ideally this would be equal to the actual ADC transition voltages but non-ideal effects like additive noise in the ADC and the test setup, phase noise in the signal generator, jitter in the sampling instant and frequency errors in the stimulus signal and sampling clock lead to values that are random. One would want those values to be unbiased, that is, their average over many test repetitions equals the actual ADC transition voltages and that their standard deviation is as low as possible.

3. Estimation Uncertainty

Here we consider only the presence of voltage noise which can be present in the stimulus signal itself or generated internally in the ADC. We represent both cases by an additive component present at the ADC input – additive noise and represent it by $n(t)$. Furthermore, here we consider this noise to be essentially of thermal origin and thus normally distributed with a null means and a standard deviation σ_r. The input signal is sampled by the ADC, as described in (3), and thus we have a set of M sampled voltages which include the stimulus signal and input equivalent random noise:

$$v_i = C - A \cdot \cos(2\pi f \cdot t_i + \varphi) + r_i \, , i = 0, 1, \dots, M-1. \quad \text{.....(5)}$$

To ease the presentation, we are going to use a normalized sample voltage given by

$$u_i = \frac{v_i - C}{A}. \quad \text{.....(6)}$$

The normalized sample voltages are thus given by

$$u_i = n_i - \cos(2\pi f \cdot t_i + \varphi) \, , i = 0, 1, \dots, M-1, \quad \text{.....(7)}$$

Where the normalized additive noise is given by

$$n_i = \frac{r_i}{A}, \quad \text{.....(8)}$$

And has a standard deviation given by

$$\sigma_n = \frac{\sigma_r}{A}. \quad \text{.....(9)}$$

The ADC transition voltages will also be normalized by dividing them by the stimulus signal amplitude A. We thus have

$$U_k = \frac{T_k}{A}. \dots\dots\dots\dots\dots\dots \quad (10)$$

We are also going to introduce the variable

$$\gamma_i = 2\pi f \cdot t_i + \varphi, \quad \text{.....(11)}$$

as the "phase" of each sample which is the argument of the cosine function in (7).

The probability that the sampled voltage is equal to or lower than the transition voltage U_k depends on the sample phase, γ_i, and the sampled voltage probability density function $f(u)$ and is given by

$$p_k(\gamma_i) = \int_{-\infty}^{U_{k+1}} f_{u_i}(u|\gamma_i) \cdot du. \quad \text{.....(12)}$$

Since we are considering the presence of null mean normally distributed random noise with standard deviation σ_n the probability density function of the sampled voltage is

$$f_{u_i}(u|\gamma_i) = \frac{1}{\sqrt{2\pi}\sigma_n} e^{\frac{-[u+\cos(\gamma_i)]^2}{2\sigma_n^2}}. \quad \text{.....(13)}$$

The probability p_k can also be written in terms of the probability distribution function,

$$F_{u_i}(U|\gamma_i) = \int_{-\infty}^{U} f_{u_i}(u|\gamma_i) \cdot du, \quad \text{.....(14)}$$

which, in the case of the normally distributed noise is equal to

$$F_{u_i}(U|\gamma_i) = \frac{1}{2} + \frac{1}{2}\,\mathrm{erf}\left(\frac{U+\cos(\gamma_i)}{\sqrt{2}\sigma_n}\right). \quad \text{.....(15)}$$

Typically, in order to increase the precision of the transition voltage estimates, many sets of M samples are acquired. Furthermore, the start of the acquisition of each set is not triggered by the stimulus signal. Consequently, we can consider the initial phase φ to be a random variable uniformly distributed in the interval from 0 to 2π. The distribution of the sampled voltages thus becomes

$$F_{u_i}(U) = \frac{1}{2\pi}\int_{-\pi}^{\pi}\left[\frac{1}{2}+\frac{1}{2}\mathrm{erf}\left(\frac{U+\cos(\gamma)}{\sqrt{2}\sigma_n}\right)\right]d\gamma. \quad \text{.....(16)}$$

Introducing now the binomial variable w_k which equals 1 if the ADC digital output code corresponding to a certain input voltage belongs to class k of the cumulative histogram and 0 otherwise. The probability density function of this variable is

$$f_{w_k}(w) = \begin{cases} p_k, & w = 1 \\ 1-p_k, & w = 0 \end{cases}, \quad \text{.....(17)}$$

Where p_k is the probability discussed earlier in (12), that is, the probability that a sample belongs to class k of the cumulative histogram. We thus have

$$p_k = P\{u \leq U_{k+1}\} = F_{u_i}(U_{k+1}). \quad \text{.....(18)}$$

The number of counts in class k of the cumulative histogram is

$$c_k = \sum_{i=0}^{M-1} w_i. \quad \text{.....(19)}$$

Note that the variables w_i are statistically uncorrelated and according to the central limit theorem the sum of a large number o random variables is normally distributed regardless of the individual distributions. We thus have that the number of counts of the cumulative histogram, c_k, is normally distributed:

$$F_{c_k} = \frac{1}{2}+\frac{1}{2}\mathrm{erf}\left(\frac{c-\mu_{c_k}}{\sqrt{2}\sigma_{c_k}}\right). \quad \text{.....(20)}$$

The variance of the number of counts of the cumulative histogram can be obtained from the probability p_k using

$$\sigma_{c_k}^2 = \mu_{\sigma_{c_k}^2} + {\sigma_{\mu}}^2_{c_k}, \quad \text{.....(21)}$$

as given in [24]. This variance is split into two terms so that we can better understand its dependence on the transition voltage and noise standard deviation. According to [24] we have

$$\mu_{\sigma_{c_k}^2} = \frac{M}{2\pi}\int_{-\pi}^{\pi} p_k(\gamma)[1-p_k(\gamma)]\cdot d\gamma, \quad \text{.....(22)}$$

and

$$\sigma_{\mu_{c_k}}^2 = \frac{M}{2\pi}\int_{-\frac{\pi}{M}}^{\frac{\pi}{M}}\left[\sum_{i=0}^{M-1} p_k\left(\frac{2\pi}{M}i+\varphi\right)\right]^2 d\varphi - \left[\frac{M}{2\pi}\int_{-\pi}^{\pi} p_k(\gamma)d\gamma\right]^2 \quad \text{.....} \qquad (23)$$

4. Number of Counts of the Cumulative Histogram as a Function of Transition Voltage and Noise Standard Deviation

We are now going to plot some charts that illustrate the dependence of the variance of the number of counts of the cumulative histogram, $\sigma_{c_k}^2$, on the transition voltage and on the additive noise standard deviation. This will eventually allow us to propose an approximate expression for that variance and ultimately for the variance of the estimated transition voltages.

The two terms into which we have split the variance of the number of counts will now be called “the mean of the variance”, $\mu_{\sigma_{c_k}^2}$, and “the variance of the mean”, ${\sigma_{\mu}}^2_{c_k}$.

In Figure 4 one can see how the variance of the mean of the number of counts of the cumulative histogram changes with the additive noise standard deviation, σ_n, for the different ADC transition voltages, U_{k+1}.For low amounts of noise the variance of the mean has a strong dependence on the transition voltage. In fact, the number arcs observed for $\sigma_n = 0$ is the same as the number of samples, M. In the present case there are five arcs because $M = 5$. As the noise standard deviation increases that dependence is lower and in the limit of large noise standard deviation that dependence in negligible and the variance of the mean goes to 0.

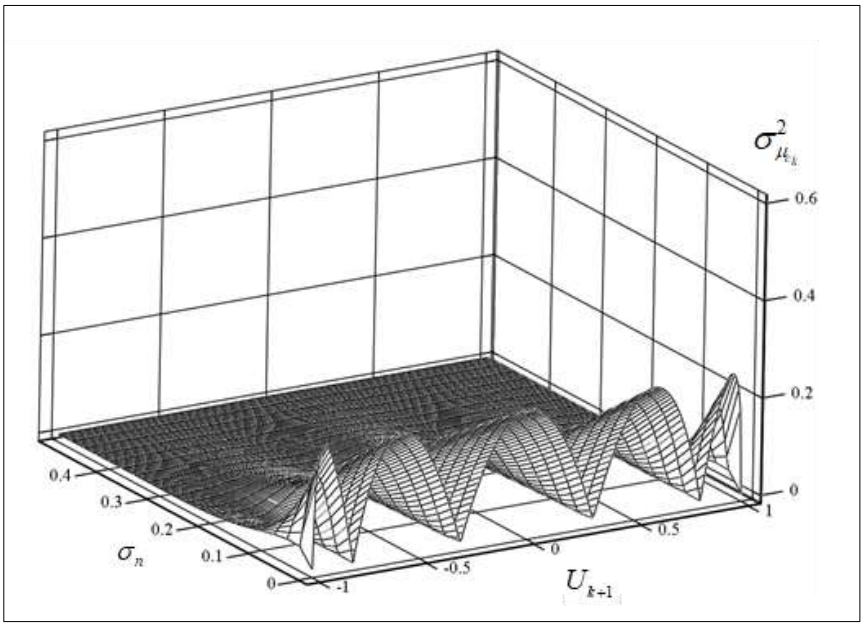

Figure 4 Variance of the mean as a function of additive noise (divided by the signal amplitude) standard deviations and transition voltage

In Figure 5 we plot the other term, the variance of the mean. In this case there is no dependence on the number of samples in the limit of null noise standard deviation. In fact, this term is null in that case. As the noise standard deviation increases so does this term, although not in a completely linear way. As we will see later that increase tops out at $M/4$.

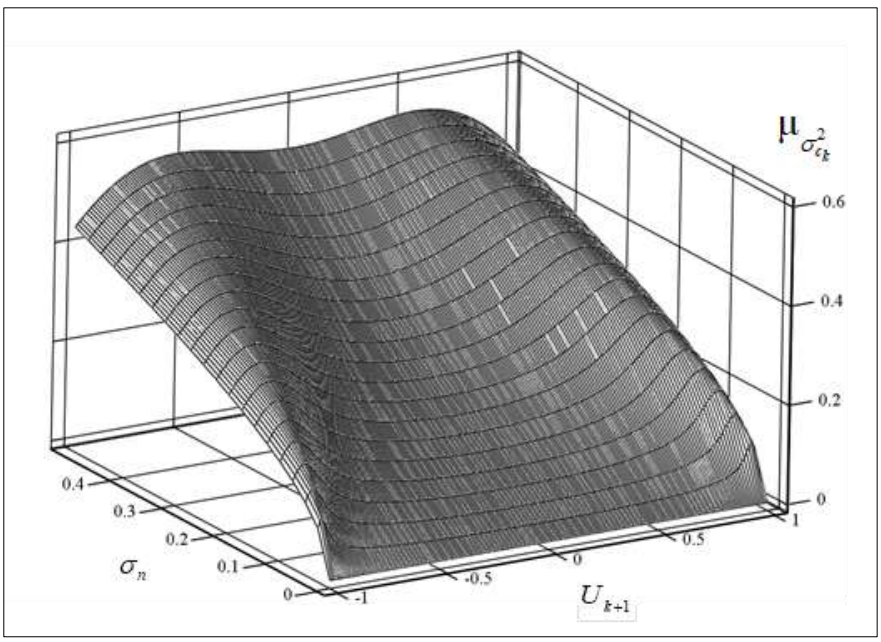

Figure 5 Mean of the variance as a function of additive noise (divided by the signal amplitude) standard deviations and transition voltage

In Figure 6 we depict the sum of those two previous charts with constitutes the variance of the number of counts of the cumulative histogram, as given by (21). Both phenomena described in the last two figures are visible: the M arcs in the case of $\sigma_n = 0$ and the increase in variance as the standard deviation of the noise increases.

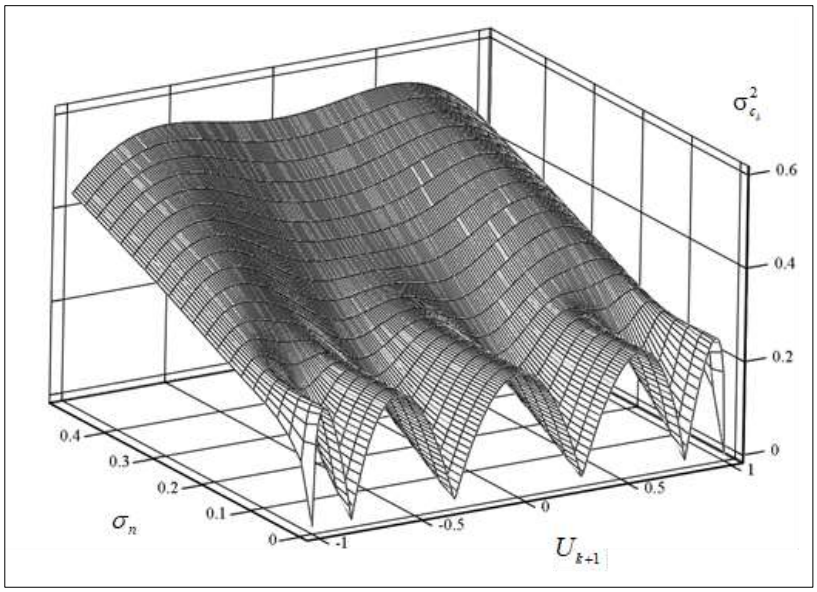

Figure 6 Variance of the number of counts of the cumulative histogram as a function of the normalized additive noise standard deviations and transition voltage

In Figure 7 we see essentially the same as in Figure 6 but we have extended the range of the additive noise standard deviation up to the normalized value of 3 which is very high amount of noise (noise standard deviation three times the stimulus signal amplitude). Here it is more easily visible the topping off of the variance of the number of counts at $M/4$.

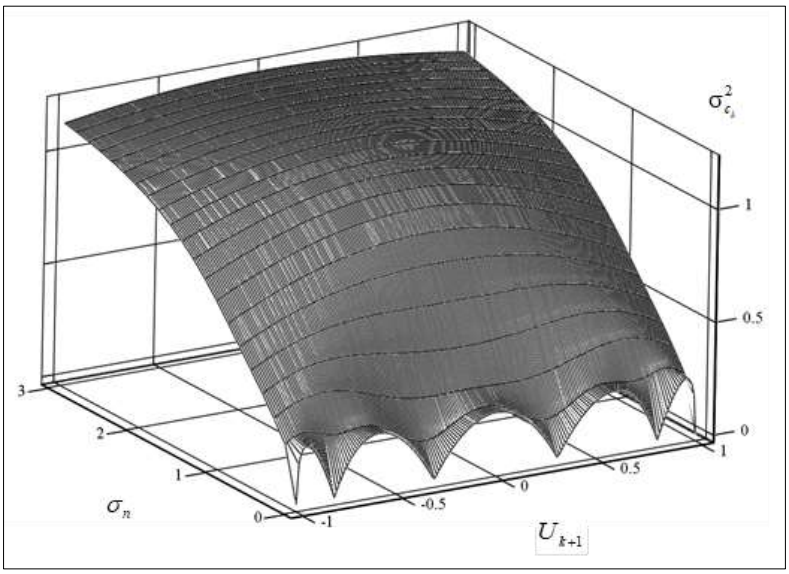

Figure 7 Variance of the number of counts of the cumulative histogram as a function of the normalized additive noise standard deviations and transition voltage for a larger range of noise

The interest in knowing the variance of the number of counts of the cumulative histogram is because it is used to estimate the ADC transition voltages, as per (4) and knowing their standard deviation allows one to build a confidence interval for the measurement made. A simple mathematical expression is thus convenient. The one already proposed in [24] is

$$\sigma_{c_k}^2 \approx \max\left(\frac{1}{4}, M \cdot \min\left(\frac{1}{4}, \frac{\sigma_n}{\pi\sqrt{\pi}}\right)\right). \quad \text{.....(24)}$$

This approximate expression does not depend on the transition voltage. Its dependence on the noise standard deviation can be observed in Figure 8.

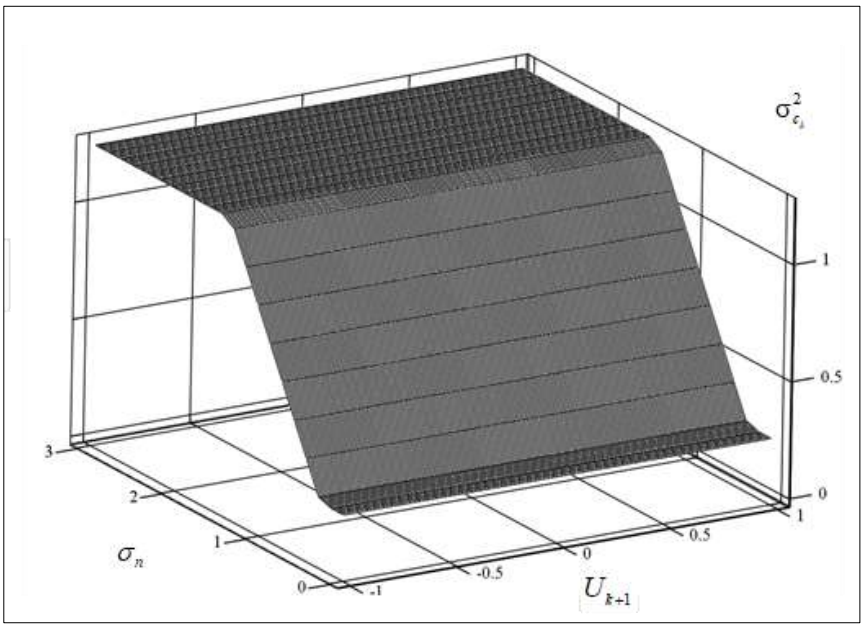

Figure 8 Approximate expression for the variance of the number of counts of the cumulative histogram as a function of the normalized additive noise standard deviations and transition voltage

One can see, from the chart in Figure 9 how the values of the approximate expression given in (24) compare with the actual values in the case of a very low number of samples and for a null transition voltage.

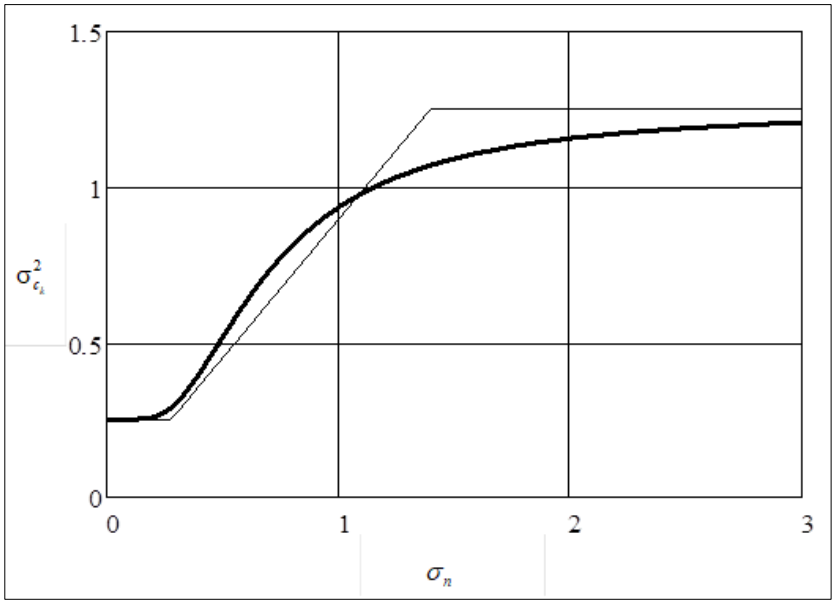

Figure 9 Number of counts of the cumulative histogram as a function of the normalized additive noise standard deviation (thick line) and approximate expression (thin line) for an acquisition of M = 5 samples (null transition voltage)

In the case of a more realistic number of samples, like 1000, one can see how the approximate analytical expression compares with the actual values in the case of three different normalized transition voltages values, namely 0, 0.6 and 0.99 in Figure 10.

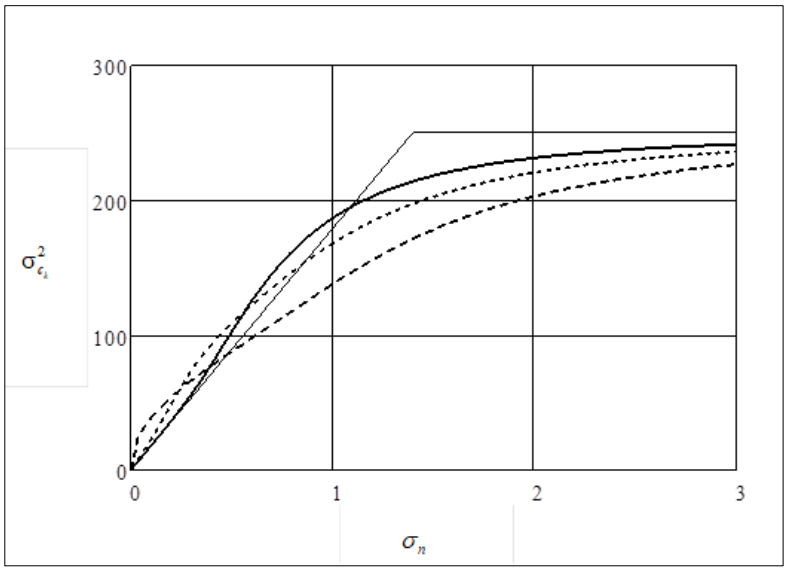

Figure 10 Number of counts of the cumulative histogram as a function of the normalized additive noise standard deviation for different values of transition voltages (solid line: U = 0, dotted line: U = 0.6, dashed line: U = 0.99) for an acquisition of M = 1000 samples. The approximate expression is represented with a solid thin line

5. Estimated Transition Voltages

The ADC transition voltages are estimated from the obtained number of counts of the cumulative histogram using (4). Employing a Tayler series approximation of that relationship one can obtains the standard deviation of the transition voltages using the first order term of the series only:

$$\sigma_{\hat{T}}^2 \approx \left(\frac{A\pi}{M}\right)^2 \cdot \sigma_{c_k}^2. \quad \text{.....(25)}$$

The proposed approximate analytical expression for the variance of the estimated transition voltages is then, from (24)

$$\sigma_{\hat{T}}^2 \approx \left(\frac{A\pi}{M}\right)^2 \cdot \max\left(\frac{1}{4}, M \cdot \min\left(\frac{1}{4}, \frac{\sigma_n}{\pi\sqrt{\pi}}\right)\right). \quad \text{.....(26)}$$

As expected, the more samples are acquired and the less noise is present, the lower is the transition voltage estimate's variance.

6. Conclusion

The study presented pertains to the case where additive normally distributed noise is present. It does not apply to other kinds of noise, like jitter, nor to noise with other statistical distributions.

The charts presented allow one to have an idea of how the cumulative histogram variance changes with number of samples, transition voltage and noise standard deviation.

Furthermore, an analytical expression be used to quickly to obtain the variance of the transition voltage estimated given the histogram test conditions is offered. Its deviation from the actual values is shown using an illustrative chart.

Compliance with ethical standards

Acknowledgments

This work was supported in by Fundação para Ciência e a Tecnologia under the research projects UIDB/50008/2020 and FCT.CPCA.2022.01 whose support the author gratefully acknowledges.

References

[1] S. Rapuano, P. Daponte, E. Balestrieri, L. de Vito, S. Tilden, S. Max, J. Blair, ADC parameters and characteristics, IEEE Instrumentation and Measurement Magazine, vol. 8, no. 5, pp. 44-54, 2005.

[2] T.E. Linnenbrink, J. Blair, S. Rapuno, P. Daponte, E., Balestrieri, L. de Vito, S. Max, S. Tilden, ADC testing, IEEE Instrumentation and Measurement Magazine, vol. 9, no. 2, pp. 39–49, 2006.

[3] F. Corrêa Alegria, P. Girão, V. Haasz, and A. Cruz Serra, Performance of Data Acquisition Systems From the User's Point of View, IEEE Transactions on Instrumentation and Measurement, vol. 53, no. 4, August 2004, pp. 907-914, https://doi.org/10.1109/TIM.2004.830757.

[4] F. Corrêa Alegria, P. Girão, V. Haasz, and A. Cruz Serra, Performance of Data Acquisition Systems From the User's Point of View, Proceedings of the IEEE Instrumentation and Measurement Technology Conference, Vail, Colorado, USA, May 2003, pp. 940-945, https://doi.org/10.1109/IMTC.2003.1207891.

[5] F.A. Corrêa Alegria, A. Moschitta, P. Carbone, A.M. da Cruz Serra, and D. Petri, Effective ADC Linearity Testing Using Sinewaves, IEEE Transactions on Circuits and Systems – Regular papers, vol. 52, no. 7, July 2005, https://doi.org/10.1109/TCSI.2005.851393.

[6] F. Corrêa Alegria and A. Cruz Serra, Uncertainty of the estimates of sine wave fitting of digital data in the presence of additive noise, IEEE Instrumentation and Measurement Technology Conference Proceedings, Sorrento, Italy, 24-27th April 2006, pp. 1643-1647.

[7] F. Corrêa Alegria, A. Cruz Serra, Uncertainty of ADC random noise estimates obtained with the IEEE 1057 standard test, IEEE transactions on instrumentation and measurement, vol. 54, no. 1, pp. 110-116, 2005, https://doi.org/10.1109/TIM.2004.840226.

[8] F. Corrêa Alegria and A. Cruz Serra, Gaussian jitter-induced bias of sine wave amplitude estimation using three-parameter sine fitting, IEEE Transaction in Instrumentation and Measurement, vol. 59, no. 9, September 2010, pp. 2328-2333, https://doi.org/10.1109/TIM.2009.2034576.

[9] Alfio Zanchi, Senior Member, Carlo Samori, Analysis and Characterization of the Effects of Clock Jitter in A/D Converters for Subsampling, IEEE Transactions on Circuits and Systems—I: Regular Papers, vol. 55, no. 2, March 2008, pp. 522-534, https://doi.org/10.1109/TCSI.2008.916576.

[10] F. Corrêa Alegria and A. Cruz Serra, Influence of Frequency Errors in the Variance of the Cumulative Histogram, IEEE Transactions on Instrumentation and Measurements, vol. 50, n. 2, April 2001, pp. 461-464, https://doi.org/10.1109/19.918166.

[11] Paolo Carbone and Giovanni Chiorboli, ADC Sinewave Histogram Testing with Quasi-choerent Sampling, Proceedings of the 17th IEEE IMTC Conference, vol. 1, pp. 108-113, May 2000, Baltimore, USA, https://doi.org/10.1109/IMTC.2000.846837.

[12] S. N. Domenico; Acoustic wave propagation in air-bubble curtains in water; Part I, History and theory. Geophysics 1982, vol. 47, no. 3, pp. 345-353. https://doi.org/10.1190/1.1441340.

[13] O. Birjukova, S. Guillén Ludeña, F. Alegria, A.H. Cardoso, Three dimensional flow field at confluent fixed-bed open channels, Proceedings of River Flow 2014, pp. 1007-1014, 2014, ISBN: 978-1-138-02674-2.

[14] O. Birjukova Canelas, R.M.L. Ferreira, S. Guillén-Ludeña, F.C. Alegria, A.H. Cardoso, Three-dimensional flow structure at fixed 70 open-channel confluence with bed discordance, Journal of Hydraulic Research, vol. 58, no. 3, pp. 434-446, 2020, https://doi.org/10.1080/00221686.2019.1596988.

[15] S. Guillén-Ludeña, M. J Franca, F. Alegria, A.J. Schleiss, A.H. Cardoso, Hydromorphodynamic effects of the width ratio and local tributary widening on discordant confluences, Geomorphology, vol. 293, pp. 289-304, September 2017, https://doi.org/10.1016/j.geomorph.2017.06.006.

[16] M. Joordens et al., Low-cost underwater robot sensor suite, 2008 IEEE International Conference on System of Systems Engineering, Monterey, CA, USA, 2008, pp. 1-6, https://doi.org/10.1109/SYSOSE.2008.4724140.

[17] R. Queirós, F.A. Corrêa Alegria, P. Silva Girão, A. Cruz Serra, A multi-frequency method for ultrasonic ranging, Ultrasonics, vol. 63, pp. 86-93, December 2015, https://doi.org/10.1016/j.ultras.2015.06.018.

[18] Esa Korhonen, Carsten Wegener, Juha Kostamovaara, Combining the Standard Histogram Method and a Stimulus Identification Algorithm for A/D Converter INL Testing With a Low-Quality Sine Wave Stimulus, IEEE Transactions on Circuits and Systems—I: Regular Papers, vol. 57, no. 6, pp. 1166-1174, June 2010, https://doi.org/10.1109/TCSI.2009.2030096.

[19] G. Chiorboli and C. Morandi, About the Number of Records to be Acquired for Histogram Testing of A/D Converters using Synchronous Sinewave and Clock Generators, in Proceedings of the 4th Workshop on ADC Modeling and Testing, Bordeaux, France, September 9-10, 1999, pp. 182-186, https://doi.org/10.1016/S0920-5489(00)00043-X.

[20] Paolo Carbone and Giovanni Chiorboli, ADC Sinewave Histogram Testing with Quasi-coherent Sampling, Proceedings of the 17th IEEE IMTC Conference, vol. 1, pp. 108-113, May 2000, Baltimore, USA, https://doi.org/10.1109/IMTC.2000.846837.

[21] A. Cruz Serra, F. Corrêa Alegria, L. Michaeli, P. Michalko, J. Saliga, Fast ADC Testing by Repetitive Histogram Analysis, IEEE Instrumentation and Measurement Technology Conference Proceedings, Sorrento, Italy, 24-27th April 2006, pp. 1633-1638, https://doi.org/10.1109/IMTC.2006.328161.

[22] IEEE Standard for Digitizing Waveform Recorders, IEEE Standard 1057-2007, April 2008, ISBN: 978-0-7381-6902-6.

[23] J. Blair, Histogram measurement of ADC non linearities using sine waves, IEEE Transactions on Instrumentation and Measurement, vol. 43, nº 3, pp. 373-383, June 1994, https://doi.org/10.1109/19.293454.

[24] F. Corrêa Alegria, A. Cruz Serra, Uncertainty in the ADC Transition Voltages Determined with the Histogram Method, Proceedings of the 6th Euro Workshop on ADC Modelling and Testing, Lisbon, Portugal, pp. 28-32, 13-14 September 2001, ISBN: 97298115-5-5.

[25] F. Corrêa Alegria, Static and Dynamic Characterization of Analog-to-digital Converters Using the Histogram Method, Ph.D. Thesis, May 2002.

[26] N. Björsell, P. Händle, Truncated Gaussian noise in ADC histogram tests, Measurement, vol. 40, no. 1, pp. 36-42, January 2007, https://doi.org/10.1016/j.measurement.2006.05.005.

[27] N. Björsell, P. Händel, Benefits with truncated Gaussian noise in ADC histogram tests, Proceeding of the Workshop on ADC Modelling and Testing, Athens, 2004.

[28] A. Moschitta, P. Carbone, D. Petri, Statistical performance of Gaussian ADC histogram test, Proceedings of the International. Workshop on ADC Modelling and Testing, pp. 213-217, 2003.

[29] F. Corrêa Alegria, A. Cruz Serra, ADC transfer curve types—A review, Computer Standards & Interfaces, vol. 28, no. 5, pp. 553-559, 2006, https://doi.org/10.1016/j.csi.2005.07.003.

[30] IEEE, Std 1241-2010 IEEE Standard for Terminology and Test Methods for Analogue-to-Digital Converters, 2010, https://doi.org/10.1109/IEEESTD.2011.5692956.